Theoretical study of topological materials

Yan Sun#, Claudia Felser, Jacob Gayles, Enke Liu, Jonathan Noky, Shu-Chun Wu, Qiunan Xu, Binghai Yan, Jakub Železný, and Yang Zhang

We have theoretically studied topological materials ranging from topological insulators to semimetals from the perspective of topological band theory. In insulators, we predicted a strong 3D Z_2 topological insulator with the largest energy gap of 0.7 eV ($BaBiO_3$), and two-dimensional large-gap quantum spin and anomalous Hall insulators based on stanene. By extending the topological band theory to metals, the linear band crossing of Weyl points behaves as the monopoles of Berry curvatures and gives rise to a new topological phase in Weyl semimetals. We have proposed the first experimentally discovered type-II Weyl semimetal in $MoTe_2$ and the first experimentally verified magnetic Weyl semimetal in $Co_3Sn_2S_2$. Since Weyl points can be only defined in three dimensions, we have obtained quantized anomalous Hall effects in the two-dimensional limit of Weyl semimetals by breaking the translation symmetry along one direction. In collaboration with colleagues, we find that the shape of surface Fermi arcs strongly depends on the spin-orbit coupling strength. The Fermi arc is a topological state and is robust against weak perturbations. We have successfully designed theoretical surface states constructed only from Femi arcs by introducing foreign atoms at the surface to saturate any dangling bonds. In bulk transport, we predicted a strong spin Hall effect in TaAs that originates from Weyl points and nodal lines. By analysing the symmetry of the Berry curvature, it was found that the anomalous Hall effect can even exist with zero net moments in the absence of the symmetry operation that changes the sign of the Berry curvature. The anomalous Hall effect can be enhanced by taking advantage of the special Weyl point band structures and nodal lines. Following this guiding direction, we have observed a strong anomalous Hall effect in Mn_3Ge/Sn non-collinear antiferromagnets. Replacing the electrical field by a temperature gradient, transverse charge current and spin current can be also observed due to the anomalous and spin Nernst effects.

Topological insulators and materials have attracted considerable attention over the last decade. The surface or edge of topological insulators are present as Dirac cone-type metallic states with helical spin texture and are protected by the topological order in the bulk band gap. The two-dimensional topological insulator behaves as a quantum spin Hall effect that is protected from time reversal symmetry. The quantum anomalous Hall insulator can be obtained by breaking time reversal symmetry and maintaining the inverted band order. In our previous studies, we mainly focused on different topological phases in insulators, such as three dimensional strong and weak topological insulators and the two-dimensional quantum spin Hall and anomalous Hall effects.

From the study of topological phases in insulators, it can be understood that topological band theory can be further generalized to metals. By combining topological band theory and symmetries, different types of topological semimetals can be defined, in which Weyl semimetals are the most robust type from the perspective of symmetry. In Weyl semimetals, bands disperse linearly in three-dimensional momentum space through the Weyl point. The Weyl node acts as a monopole with fixed chirality and acts as a source or a sink of the Berry curvature. Since the topological charge is only locally defined in Weyl semimetals, the surface

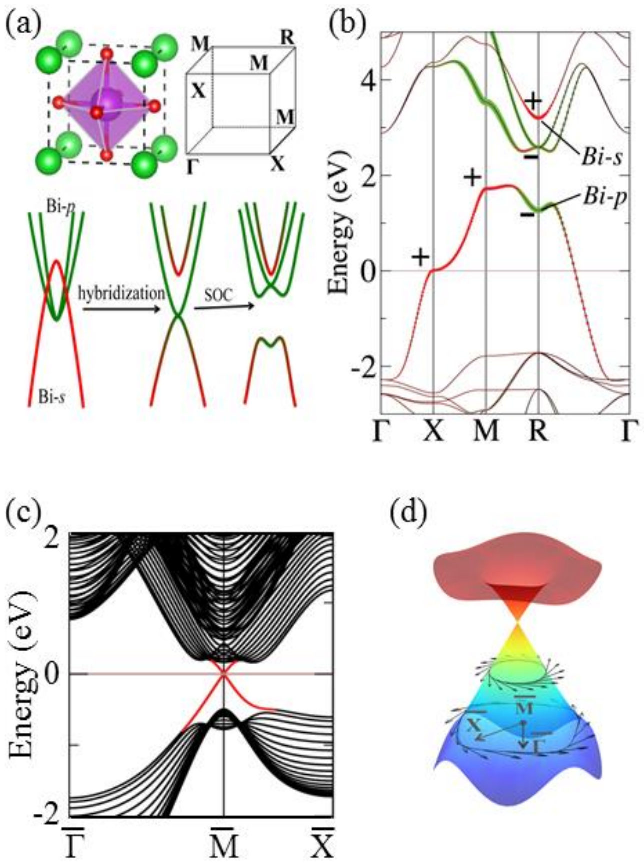

Fig.-1: (a) $BaBiO_3$ perovskite superconductor as a 3D TI with large energy gap. (b) Bulk and surface band structures. (c, d) Dirac-cone-like surface states.

states are present as open Fermi arcs. In addition, owing to the special band structures, topological semimetals often host large Berry curvature in momentum space, leading to special bulk transport properties. Although the Berry curvature is odd with respect to time reversal, the spin-projected Berry curvature is even. Therefore, strong spin Hall and anomalous Hall effect are expected to occur in nonmagnetic and magnetic topological semimetals, respectively. The interplay between Berry curvature and lattice symmetry in magnetic materials allows the existence of the anomalous Hall effect, even with vanishing net magnetic moments, and the signals are strongly enhanced by the topological band structures

3D TI BaBiO3 with the largest energy gap

The band gap in topological insulators is purely due to the intrinsic SOC split. The Bi-6p states exhibit probably the largest intrinsic SOC split. Therefore, we may use Bi to design a TI with the largest recorded band gap. We choose the famous perovskite $BaBiO_3$, which is known to be a superconductor in the hole-doping case (T_c ~ 30 K). We found that a large band gap (more than 1 eV) opens due to SOC in the electron-doped region with simultaneous band inversion, which has been omitted for decades in previous studies. As a consequence, we found a 3D TI in this material with an indirect energy gap of 0.7 eV (see Fig. 1), which is the largest gap among all known 3D TIs [1].

Stanene as the first large-gap 2D TI and room-temperature QAH insulator

(i) While collaborating with the Prof. Shou-Cheng Zhang's group at Stanford, we found that a Sn honeycomb layer with dangling-bond passivation mimics the simplest case of a 2D monolayer of the KHgSb-type weak TIs. The two dimensional Sn lattice, called stanene in analogue to graphene, exhibits 0.3 ~ 0.4 eV energy gap (see Fig. 2 (a)) [2], which is orders of magnitude larger than that of HgTe quantum wells. The stanene layer has been successfully grown by the MBE technique [F. Zhu et al. Nat. Mater., 14,

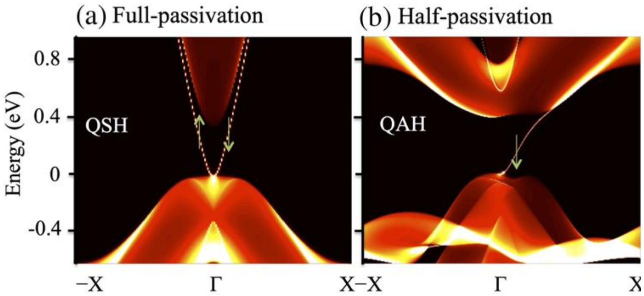

Fig.-2: Edge states for (a) quantum spin Hall and (b) quantum anomalous Hall insulators in a 2D Sn lattice with and without I passivation, respectively.

1020 (2015)] and the topological edge states await further identification.

(ii) The large-gap two-dimensional topological insulator encourages us to design a large-gap QAH insulator by introducing FM doping. We propose a simple method for fabricating stable FM order by passivation of only half of the stanene lattice. Subsequently, strong exchange coupling drives the two dimensional TI into the QAH phase (see Fig. 2(b)). The large energy-gap (0.3 eV) and high T_c value of the FM order promise a novel QAH system that can function near room temperature [3].

Topological Fermi arcs in Weyl semimetals

Based on our high quality single crystals and with the support from our accurate ab initio calculations [4-5], our close collaborator Prof. Yu-Lin Chen at Oxford clearly observed Fermi arcs on the surface and bulk linear band crossings in TaAs [4]. We successfully distinguished the Fermi arcs from the trivial dangling bond states using spin texture analysis (Fig. 3 (a-b)). The observation of unique surface Fermi arcs and the bulk Weyl points with linear dispersion together with the overall agreement between measurements and theoretical calculations (Fig. 3 (c-d)) establish TaAs as

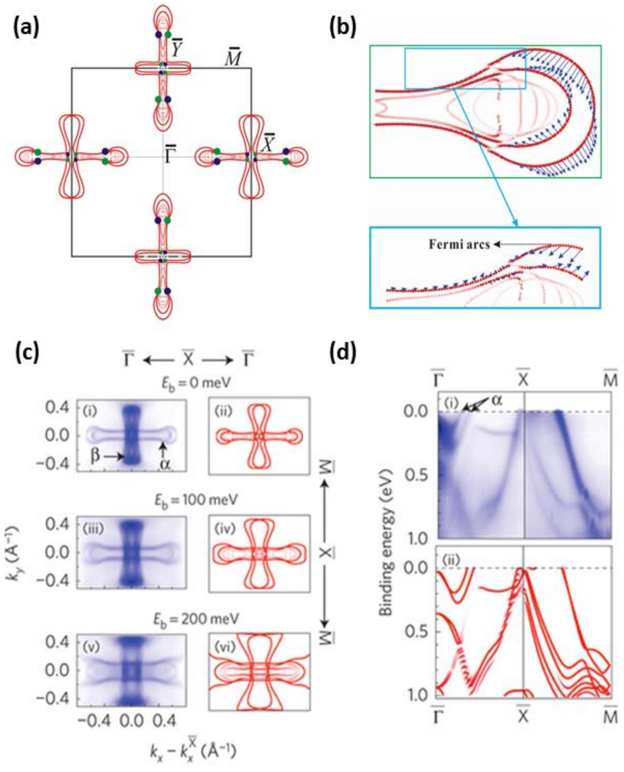

Fig.-3: (a) 2D Fermi surface of TaAs in the 001 plane from ab-initio calculations. (b) Spin texture of the Fermi surface. (c, d) Agreement between ARPES measurements and our calculations for the Fermi surfaces and band structures.

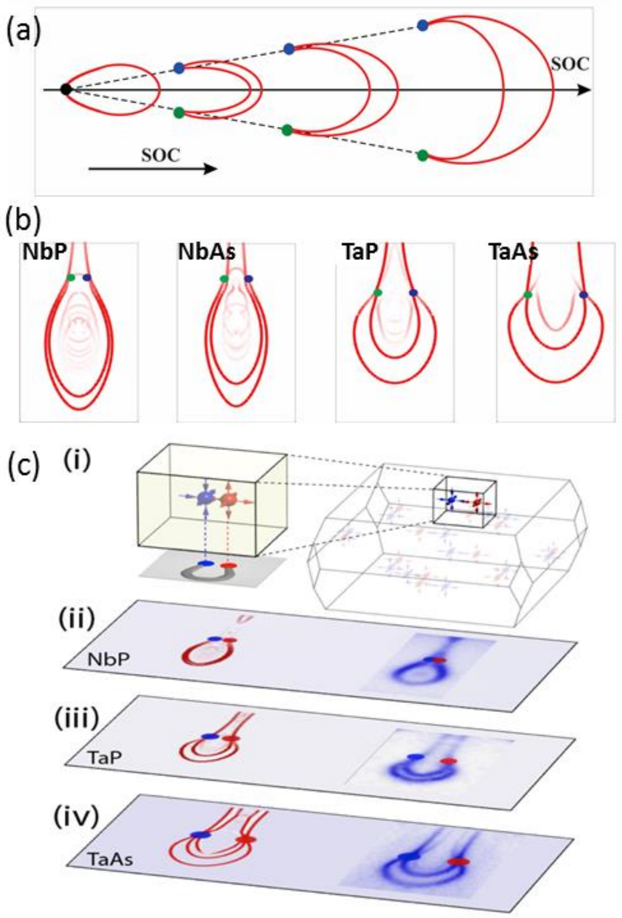

Fig.-4: (a) Schematic diagram of the Fermi arcs with increasing SOC strength. (b) Calculated Fermi arcs in NbP, NbAs, TaP, and TaAs. (c) Comparison of the Fermi arcs from calculations (left) and ARPES measurements (right).

the first Weyl semimetal experimentally observed. The discovery of this family of Weyl semimetals provides a rich material base for exploring many exotic physical phenomena and novel future applications.

By systematically investigating Fermi arcs in NbP, TaP, NbAs, and TaAs, we found that the Fermiology of their Fermi arcs are strongly dependent on the spin-orbit coupling strength [5, 6]. Without the inclusion of spin-orbit coupling, the Fermi surface exists as a closed Fermi circle. As long as spin-orbit coupling effect is taken into consideration, the spin-degenerate point is lifted into one pair of Weyl points with opposite chirality following mirror symmetry. Meanwhile, the Fermi circle is transformed into an open Fermi arc terminated at two Weyl points (Fig. 4(a)). Splitting between the positive and negative Weyl points also increases as the spin-orbit coupling strength increases (Fig. 4). This discovery and the spin orbit coupling controlled band structure and Fermiology tuning further pave the way for the exploration of novel

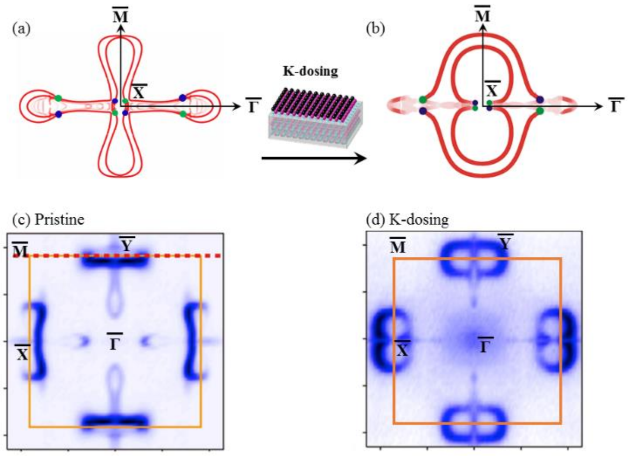

Fig.-5: Simple Fermi arcs were observed after the Lifshitz transition with potassium deposition on the surface of NbAs. Our calculations (a-b) were verified with ARPES measurements (c-d).

phenomena and potential future applications in Weyl semimetals.

Since the Fermi arc is a topological state, it is robust against weak perturbations. We successfully designed theoretical surface states constructed only from Femi arcs by introducing foreign atoms at the surface to saturate any dangling bonds (Fig. 5(a-b)) [6]. This enabled us to obtain pure Fermi arc states. This also enabled us to tune the detailed shape of the Fermi arcs, which is useful both for their detection and their manipulation. This theoretical proposal was observed experimentally in recent ARPES measurements, as presented in Fig. 5(c-d).

The first experimentally discovered type-II Weyl semimetal in orthorhombic $MoTe_2$

After reports of Weyl semimetals in transition metal pnictides, it was soon realised that Weyl semimetals can be classified into two groups. These are the type-I group that respects Lorentz symmetry and the type-II group that does not [Alexey A. Soluyanov, ect. Nature, 527, 495 (2015]. The volume of the Fermi surface shrinks to almost zero at conventional type-I Weyl points, whereas the Dirac cone is tilted so that there are both electron and hole Fermi surfaces at type-II Weyl points, as shown in Fig. 6(a-b).

Via first principles calculations and Berry curvature analysis, we predicted the existence of a type-II Weyl semimetal in a layered material of orthorhombic $MoTe_2$, with four pairs of Weyl points lying in the k_z=0 plane slightly above the Fermi level [7], as illustrated in Fig. 6 (c-d). Owing to the large separation between Weyl points, the surface fermi arcs are very easily detected in experiments, and hence $MoTe_2$ attracted

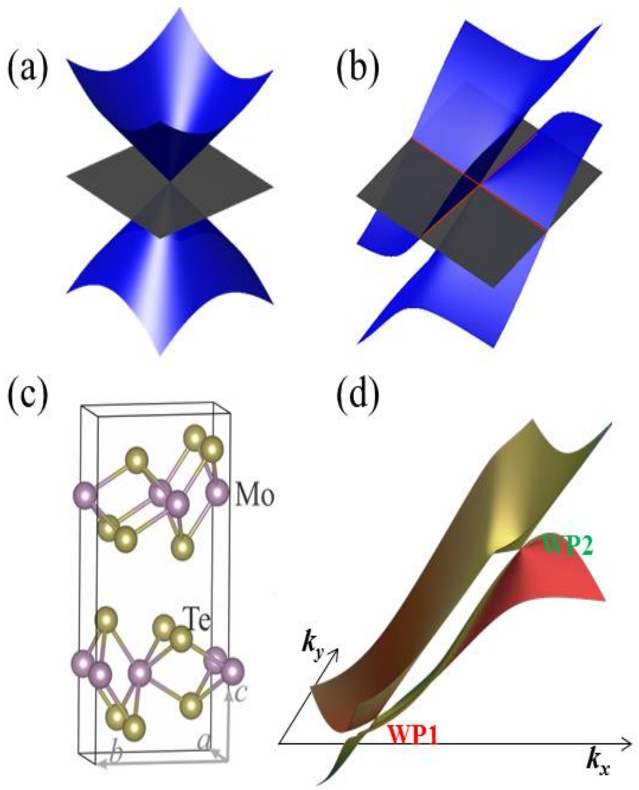

Fig.-6: (a, b) Schematic of type-I and type-II Weyl points. (c) Lattice structure and (d) type-II Weyl points in $MoTe_2$.

attention soon after our prediction. In addition, we found that the shape of the Weyl points and surface Fermi arcs in $MoTe_2$ are very sensitive to the correlation effect and lattice strain.

Over the following two years, our prediction of a type-II Weyl semimetal in T_d-$MoTe_2$ was independently verified by different groups [Nat. Phys. 12, 1105 (2016), Nat. Mater. 15, 1151 (2016) , Nat. Comm. 8, 13973 (2017)]. Fig. 7 shows that our *ab initio* calculations and ARPES measurements from our collaborators from Oxford agree well [8].

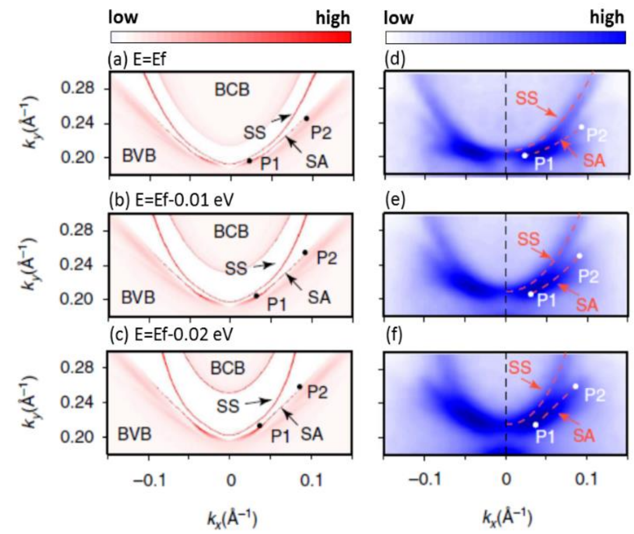

Fig.-7: (a–c) Calculated evolution of the projection of Fermi arcs. The regular surface state and surface Fermi arc are labelled SS and SA, respectively; points P1 and P2 indicate the starting and ending points of the surface Fermi arcs. (e–g) Photoemission intensity map in the same area as in (a)–(c). The dashed lines show the surface state (SS) and the surface Fermi arcs (SA).

Spin Hall effect in topological semimetals with time reversal symmetry

Besides the topological surface state, a topological semimetal also shows exotic bulk transport properties. Our *ab initio* calculations reveal a large spin Hall conductivity in the TaAs family of Weyl materials (see Fig. 8). The SHE originates intrinsically from the SOC-gapped nodal lines and Weyl points [9], which exhibit a large Berry curvature, thus the bulk carrier problem in topological insulators is naturally avoided. Considering the low charge conductivity in semi-metals, Weyl semimetals are believed to present a larger spin Hall angle. The interplay between topological band structures and the spin Hall effect suggests a new guiding direction for searching for strong anomalous Hall effect materials and topological nodal line semimetals. Using this idea, we have successfully explained the origin of the strong spin Hall effect in metallic rutile oxides.

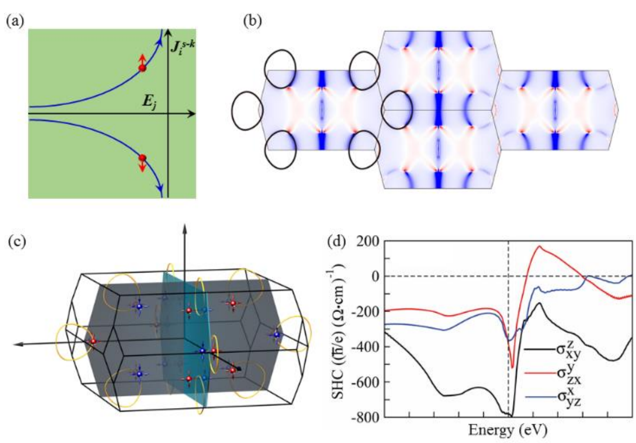

Fig.-8: (a) Schematic of the spin Hall effect. A transverse net spin current (Jis-k) is induced by a longitudinal electrical field (Ej). (b) Spin Berry curvature distribution in TaAs, which is primarily due to SOC-opened nodal lines. (c) Weyl points and nodal line distribution in the Brillouin zone. (d) Energy dependent spin Hall conductivity.

Strong anomalous Hall effect in a ferromagnetic Weyl semimetal

Today we have identified several Weyl semimetals that rely on broken inversion symmetry ranging from TaAs to $MoTe_2$. There were no counterpart magnetic Weyl semi-metals that rely on broken time reversal symmetry. In collaboration with our experimental colleagues [Enke Liu, et. al.], we proposed a promising magnetic Weyl semimetal ($Co_3Sn_2S_2$) with clean band structure and Weyl point very close to Fermi level [10]. Thus, the Weyl node related physics in $Co_3Sn_2Se_2$ should be prominent and easy to detect in experiments. We observed a strong anomalous Hall effect in this compound, which was already a hint of nodal lines and Weyl points close to the Fermi level (see Fig. 9). Owing to the significantly enhanced Berry curvature arising from the Weyl bands and its low charge conductivity, the anomalous Hall conductivity and anomalous Hall angle are very high, ~1100 S/cm and 20%, respectively. Due to the quasi-two-dimensional lattice structure and out-of-plane net magnetization, $Co_3Sn_2Se_2$ is also a promising candidate for exhibiting the quantum anomalous Hall effect. These findings provide an important indication that time-reversal-breaking half-metallic Weyl semimetals with gapped nodal lines close

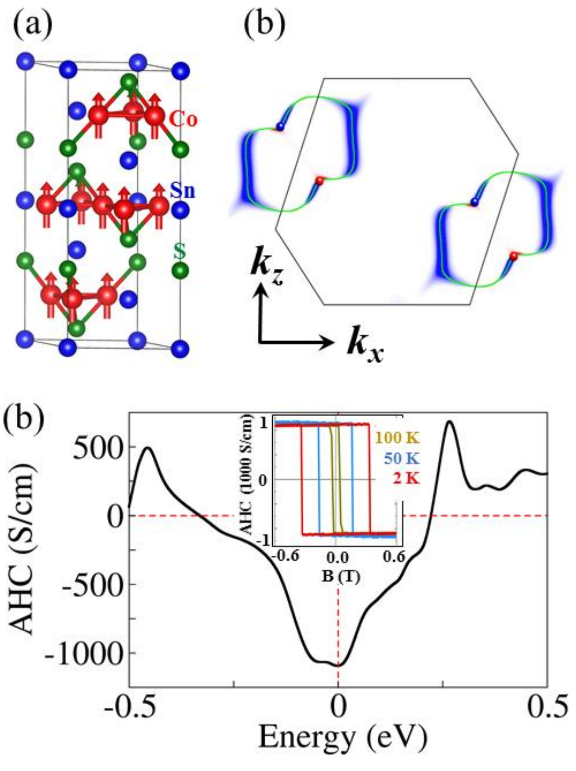

Fig.-9: (a) Lattice and magnetic structure of $Co_3Sn_2S_2$. (b) Berry curvature in $Co_3Sn_2S_2$ is primarily due to SOC-opened nodal lines. (c) Energy dependent anomalous Hall conductivity in $Co_3Sn_2S_2$. The inset shows the experimental Hall measurement.

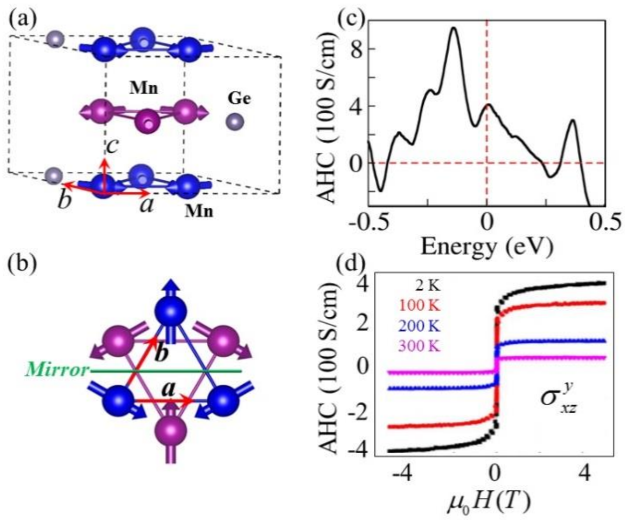

Fig.-10: (a, b) Lattice and magnetic structure for Mn_3Ge. (c) Anomalous Hall conductivity from calculation and (d) Hall measurement at different temperatures.

to the Fermi energy can host large anomalous Hall conductivities.

Because of the imbalance between spin-up and spin-down electrons in ferromagnets, the anomalous Hall effect is normally assumed to be proportional to the net magnetization. While from the analysis of symmetry of Berry curvature, the intrinsic anomalous Hall effect is allowed as long as the symmetry operations that change the sign of Berry curvature are absent. The non-zero anomalous Hall effect in antiferromagnets was proposed as early as 2001 [Shindou, R. and Nagaosa, N., Phys. Rev. Lett. 87, 116801 (2001)]. However, its experimental realisation was not successful until 2016. In collaboration with our experimental colleagues [Ajaya, et. al.], we observed strong AHE at room temperature in Mn3Ge [11] (see Fig. 10). One can see that the AHC does not scale with the magnetization, unlike conventional ferromagnets. With a small applied magnetic field, the staggered moments of antiferromagnetic order rotate, changing the sign of the AHE. In addition to the anomalous Hall effect, we have also found another interesting phenomenon in noncollinear antiferromagnets [12]: the charge current is spin polarized.

From magnetic Weyl semimetal to quantum anomalous Hall effect

The quantum anomalous Hall effect and magnetic Weyl semimetals are topological states induced by intrinsic magnetic moments and spin-orbit coupling. Since the Weyl point can only be defined in three dimensions, it is possible to evoke the quantum anomalous Hall effect by dimensional confinement of a magnetic Weyl semimetal along one direction. In the

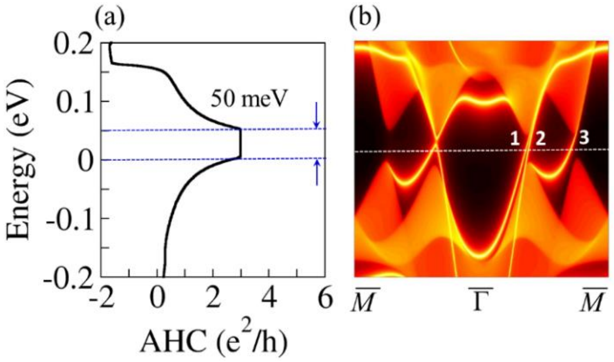

Fig.-11: Quantum anomalous Hall conductivity in the two-dimensional limit of $Co_3Sn_2S_2$. (a) Quantized anomalous Hall conductivity in the band gap with Chern number 3. (b) Three chiral edge states connect to bulk valence and conduction bands.

two-dimensional limit of $Co_3Sn_2S_2$, two QAHE states exist depending on the stoichiometry of the two-dimensional layer [13]. One is a semimetal with a Chern number of 6, and the other is an insulator with a Chern number of 3. The latter has a band gap of 0.05 eV (see Fig. 11), which is much larger than that in magnetically-doped topological insulators. Since intrinsic ferromagnets normally have a higher magnetic ordering temperature than dilute magnetic semiconductors, the quantum anomalous Hall effect obtained from this Weyl semimetal should be stable up to a higher temperature. This temperature stability is one of the most important parameters for further applications of the quantum anomalous Hall effect.

Future Plans

(i) We have identified the principles that govern interactions the between anomalous Hall (or spin Hall) effect and topological band structures. Guided by these principles, many more promising anomalous Hall and spin Hall materials can be designed. In collaboration with Prof. Stuart Parkin in MPI Halle, we will perform both theoretical and experimental investigations based on these materials.

(ii) Extending electronic transport into thermal transport, we hope to find a general relation between the topological band structure and anomalous and spin Nernst effects. We will systematically invest our ideas in collaboration our experimental colleagues Johannes Gooth et. al.

(iii) Since the quantum anomalous Hall effect does not require the quantized Landau level, it is possible to observe the quantum anomalous Hall effect in three dimensions. We will focus on two primary directions. One involves native magnetic insulators, and the other is to attempt doping non-magnetic Z_2 and high order topological insulators.

(iv) To date, the existence of magnetic Weyl semimetals only has implications on transport, whereas the direct surface Fermi arc lacks experimental proof. Our predicted quasi two-dimensional magnetic Weyl semimetal $Co_3Sn_2S_2$ provides a good platform for the surface study, due to its clean band structure [14]. We will attempt further detection of its surface Fermi arc states with ARPES and STM in collaboration with Prof. Yulin Chen from Oxford University and Prof. Haim Beidenkopf from Weizmann Institute of Science.

External Cooperation Partners

S. S. P. Parkin (Max Planck Institute of Microstructure Physics, Halle, Germany); Y. Chen (Physics Department, Oxford University, UK)

References

[1]* *A large-energy-gap oxide topological insulator based on the superconductor $BaBiO_3$, B. Yan, M. Jansen and C. Felser, Nat. Phys.* ***9*** *(2013) 709.*

[2]* *Large-Gap Quantum Spin Hall Insulators in Thin Films, Y. Xu, B. Yan, H.-J. Zhang, J. Wang, G. Xu, P. Tang, W. Duan and S.-C. Zhang, Phys. Rev. Lett.* ***111*** *(2013) 136804.*

[3]* *Prediction of Near Room Temperature Quantum Anomalous Hall Effect on Honeycomb Materials, S.-C. Wu, G. Shan and B. Yan, Phys. Rev. Lett.* ***113*** *(2014) 256401.*

[4]* *Weyl semimetal phase in the non-centrosymmetric compound TaAs, L. X. Yang, Z. K. Liu, Y. Sun, H. Peng, H. F. Yang, T. Zhang, B. Zhou, Y. Zhang, Y. F. Guo, M. Rahn, D. Prabhakaran, Z. Hussain, S.-K. Mo, C. Felser, B. Yan and Y. L. Chen, Nat. Phys.* ***11*** *(2015) 728.*

[5]* *Topological surface states and Fermi arcs of the noncentrosymmetric Weyl semimetals TaAs, TaP, NbAs, and NbP, Y. Sun, S.-C. Wu and B. Yan, Phys. Rev. B,* ***92*** *(2015) 115428.*

[6]* *Evolution of the Fermi surface of Weyl semimetals in the transition metal pnictide, Z. K. Liu, L. X. Yang, Y. Sun, T. Zhang, H. Peng, H. F. Yang, C. Chen, Y. Zhang, Y. F. Guo, D. Prabhakaran, M. Schmidt, Z. Hussain, S.- K. Mo, C. Felser, B. Yan and Y. L. Chen, Nat. Mater.* ***15*** *(2016) 27.*

[7]* *Prediction of Weyl semimetal in orthorhombic $MoTe_2$, Y. Sun, S.-C. Wu, M. N. Ali, C. Felser and B. Yan, Phys. Rev. B.* ***92*** *(2015) 161107(R).*

[8]* *Signature of type-II Weyl semimetal phase in $MoTe_2$, J. Jiang, Z. K. Liu, Y. Sun, H. F. Yang, C. R. Rajamathi, Y. P. Qi, L. X. Yang, C. Chen, H. Peng, C.-C. Hwang, S. Z. Sun, S.-K. Mo, I. Vobornik, J. Fujii, S. S. P. Parkin, C. Felser, B. H. Yan and Y. L. Chen, Nat. Comm.* ***8*** *(2016) 13973.*

[9]* *Strong Intrinsic Spin Hall Effect in the TaAs Family of Weyl Semimetals, Y. Sun, Y. Zhang, C. Felser and B. Yan, Phys. Rev. Lett.* ***117*** *(2016) 146403.*

[10]* *Giant anomalous Hall angle in a half-metallic magnetic Weyl semimetal, E. Liu, Y. Sun, L. Müchler, A. Sun, L. Jiao, J. Kroder, V. Süß, H. Borrmann, W. Wang,*

W. Schnelle, S. Wirth, S. T. B. Goennenwein and C. Felser, arXiv:1712.06722.

[11]* *Large anomalous Hall effect driven by a nonvanishing Berry curvature in the noncolinear antiferromagnet* Mn_3Ge*, A. K. Nayak, J. E. Fischer, Y. Sun, B. Yan, J. Karel, A. C. Komarek, C. Shekhar, N. Kumar, W. Schnelle, J. Kübler, C. Felser and S. S. P. Parkin, Sci. Adv.* ***2*** *(2016) e1501870.*

[12]* *Spin-Polarized Current in Noncollinear Antiferromagnets, J. Železný, Y. Zhang, C. Felser and B. Yan, Phys. Rev. Lett.* ***119*** *(2017) 187204.*

[13]* *Prediction of quantum anomalous Hall effect from a magnetic Weyl semimetal, L. Muechler, E. Liu, Q. Xu, C. Felser and Y. Sun, arXiv:1712.08115.*

[14]* *Topological surface Fermi arcs in the magnetic Weyl semimetal* $Co_3Sn_2S_2$*, Q. Xu, E. Liu, W. Shi, L. Muechler, J. Gayles, C. Felser and Y. Sun, Phys. Rev. B* ***9*** *(2018)* ***7****235416.*

ysun@cpfs.mpg.de